

Measuring Rail Seat Pressure Distribution in Concrete Crossties

Experiments with Matrix-Based Tactile Surface Sensors

Christopher T. Rapp, Marcus S. Dersch, J. Riley Edwards,
Christopher P. L. Barkan, Brent Wilson, and Jose Mediavilla

A sustained increase in gross rail loads and cumulative freight tonnages as well as growing interest in high-speed passenger rail development is placing an increasing demand on North American railway infrastructure. To meet this demand, improvements to the performance and durability of concrete crossties and fastening systems are necessary. One of the typical failure modes for concrete crossties in North America is rail seat deterioration, and researchers have hypothesized that localized crushing of the concrete in the rail seat is one of the potential mechanisms that contributes to this failure mode. To understand this mechanism better, the University of Illinois at Urbana–Champaign is using a matrix-based tactile surface sensor to measure and quantify the forces and pressure distribution acting at the contact interface between the concrete rail seat and the bottom of the rail pad. Preliminary data collected during laboratory experimentation have shown that a direct relationship existed between rail pad modulus and maximum rail seat pressure. In addition, under a constant vertical load, a direct relationship between the lateral-to-vertical force ratio and the maximum field side rail seat pressure was observed. Given that all preliminary results indicate that various combinations of pad modulus, track geometry, and lateral-to-vertical force ratio create localized areas of high pressure, crushing remains a potential mechanism leading to rail seat deterioration. Through the analysis of rail seat pressure data, valuable insight can be gained that can be applied to the development of designs for concrete crosstie and fastening system components that meet current and projected service demands.

Concrete crossties are typically used in locations that place high loading demands on the railroad track structure, necessitate stringent geometric tolerances, or both. In North America, they were adopted in response to the inability of timber crossties to perform satisfactorily in certain severe service conditions, such as areas of high curvature, heavy-axle-load freight traffic, high-speed passenger train traffic, high annual gross tonnages, steep grades, and severe climatic

conditions including areas of high moisture that would cause accelerated decay of timber ties (1). The cast-in shoulders and molded rail seat of concrete crossties increase their ability to hold gage under these loading conditions (1).

Concrete crossties are not without their design and performance challenges. As reported in surveys conducted by the University of Illinois at Urbana–Champaign (UIUC) in 2008 and 2012, North American Class I railroads and other railway infrastructure experts ranked rail seat deterioration (RSD) as one of the most critical problems associated with performance of the concrete crossties and fastening system (2, 3). Problems that arise from the deterioration of the concrete rail seat surface include widening of gage, reduction in the clamping force (toe load) of fastening clips, and insufficient rail cant (2). All of these problems have the potential to create unsafe operating conditions and an increased risk of rail rollover derailments (4).

A suspected cause of RSD is high forces acting on the concrete rail seat surface, often in concentrated areas. To address this problem, a study was performed by the John A. Volpe National Transportation Systems Center on the effect of wheel and rail loads on concrete tie stresses and rail rollover. The study confirmed the possibility of concentrated loads producing stresses exceeding the 7,000-psi (48,260-kPa) minimum design compressive strength of concrete as recommended by the American Railway Engineering and Maintenance-of-Way Association [AREMA (4)].

The combination of static wheel loads and dynamic impact loads imparts forces into the rail seat that potentially damage the concrete surface (5). The magnitude of these loads can vary on the basis of track support variations, wheel defects, or rail irregularities (5). Well-maintained concrete crosstie track is typically stiffer than timber crosstie track. According to the *AREMA Manual for Railway Engineering*, the typical track modulus value for mainline concrete crosstie track is 6,000 lb/in² (41.4 N/mm²), which is twice the typical timber crosstie track modulus of 3,000 lb/in² (20.7 N/mm²) (6). A track superstructure that is stiffer, consisting of the rail, fastening system components, and crossties, produces a less resilient response to impact loads, resulting in the transfer of higher forces to the concrete rail seat surface. This theory assumes that the track substructures, consisting of the subballast and ballast layers, for both concrete and timber crosstie track provide adequate support conditions for each track type (7). Despite the superstructure's being less resilient, a study performed to investigate the effect of replacing defective timber crossties with concrete crossties yielded results showing a drastic improvement on the remaining life of other crossties for this given section of track (8). A stiffer track structure may also be desired

C. T. Rapp, M. S. Dersch, J. R. Edwards, and C. P. L. Barkan, Rail Transportation and Engineering Center, Department of Civil and Environmental Engineering, University of Illinois at Urbana–Champaign, 205 North Mathews Avenue, Urbana, IL 61801. B. Wilson, Amsted Rail, Inc., 1700 Walnut Street, Granite City, IL 62040. J. Mediavilla, Amsted RPS, 8400 West 110th Street, Suite 300, Overland Park, KS 66210. Corresponding author: C. T. Rapp, ctrapp3@illinois.edu.

Transportation Research Record: Journal of the Transportation Research Board, No. 2374, Transportation Research Board of the National Academies, Washington, D.C., 2013, pp. 190–200.
DOI: 10.3141/2374-22

for construction in an attempt to reduce permanent deformation and maintenance costs (9).

To better understand the forces acting at the concrete rail seat surface, researchers at UIUC are using matrix-based tactile surface sensors (MBTSS) as a means to measure load magnitude and distribution. MBTSS have been previously used in experimentation under the tie plates on timber crossties (10); however, researchers at UIUC are using this technology to explore the pressure distribution on the rail seats of concrete crossties.

BACKGROUND

Many factors affect the rail seat pressure distribution, one of which is the transfer of forces at the wheel–rail interface. The transfer of forces from the wheel to the rail is heavily dependent on frictional characteristics at this interface, such as the presence of top-of-rail friction modifiers (11). After the load is transferred from the wheel to the rail, it moves through the web of the rail and into the base. Next, the load is distributed through the rail pad assembly onto the rail seat of the crosstie.

The profile of the wheel and rail (e.g., the wear pattern) and the performance of the rail car truck are some of the variables that can govern the location and angle of the resultant force. The authors suspect that these parameters can cause significant variation in which areas of the rail seat are receiving concentrated loadings. In addition, the lateral-to-vertical (L/V) ratio of this resultant force also varies greatly depending on track geometry conditions. Lateral forces imparted onto the rail can be significant in horizontal curves or special trackwork. Trains traveling at speeds above or below the balancing speed of a curve can cause shifts in the vertical and lateral load to the high or low rail, respectively. These loads being imparted into the track structure are highly dependent on the speed at which a train is operating through the curve, and it is understood that trains do not always travel at the design balance speed (12). These loading scenarios are especially likely on shared infrastructure where both freight and passenger trains operate on the same track, typically at different speeds. In some cases passenger trains may operate from 25% to 35% faster than conventional traffic around curves (13). Passenger trains operating at higher speeds on a track designed primarily for freight traffic would be operating at a cant deficiency, in

which axle loads are not evenly distributed between even rails and forces on the high rail and fastening system components are higher. As a result, shared infrastructure presents diverging engineering requirements for track that can accommodate the heavy axle loads of slower-speed freight trains with the possibility of high dynamic loads from higher-speed passenger trains.

Design of the fastening system components also plays a crucial role in the distribution of pressure in the rail seat. Given the stiff nature of concrete crosstie track, the fastening system must provide some of the resiliency necessary to attenuate loads without damaging the concrete (14). Some of the variables potentially affecting the magnitude and distribution of pressure on the concrete rail seat are explored through laboratory experimentation. Preliminary results from these experiments are documented here.

SENSOR TECHNOLOGY AND PROTECTION

The sensor technology UIUC is currently using for quantifying forces and pressure distribution at the rail seat is the MBTSS manufactured by Tekscan Inc. For protection of the MBTSS from shear forces and puncture, both sides are covered with thin layers of polytetrafluoroethylene and biaxially oriented polyethylene terephthalate [BoPET (Figure 1)]. Calibration of MBTSS is conducted by applying known loads and correlating the loads with the respective raw sum units. Known input loads can also be applied to collected MBTSS data in order to quantify pressure distributions.

EXPERIMENTAL SETUP

UIUC's experimental testing was performed at the University of Illinois Advanced Transportation Research and Engineering Laboratory. The pulsating-load testing machine (PLTM), which is owned by Amsted RPS and was designed to perform AREMA Test 6 (Wear and Abrasion) and other experiments related to concrete crossties and fastening systems, was used to execute the experiments. The PLTM consists of one horizontal and two vertical actuators, both attached to a steel loading head that encapsulates a 24-in. (610-mm) section of rail. The rail section is attached to one of the two rail seats on a concrete crosstie. Preliminary UIUC research included installing a

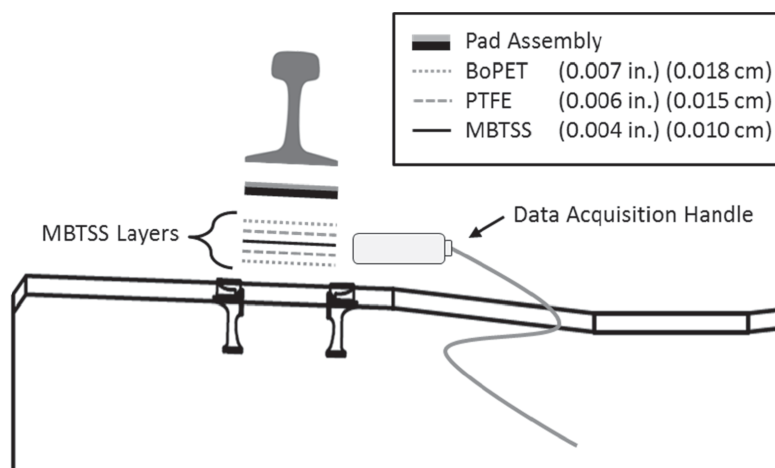


FIGURE 1 Profile view of MBTSS layers and thicknesses (PTFE = polytetrafluoroethylene).

MBTSS in the concrete crosstie fastening system and loading the tie with the PLTM. Loading inputs for this experimentation are applied to the rail in only the vertical and lateral directions because of the constraints of the experimental setup. UIUC researchers recognize that moving wheel loads impart longitudinal forces onto the track structure that add a higher level of complexity to analysis of loads on the various track components. Although it is possible that the longitudinal forces would have a large effect on varying the pressure distribution at the rail seat, the ability to simulate such loads with this experimental setup does not currently exist.

RESULTS OF EXPERIMENTATION

Experiments have been conducted by UIUC researchers to collect data on the distribution of pressure on the concrete crosstie rail seat based on expected loading conditions at the rail seat surface. The experimental setup is not meant to replicate the common field loading conditions but is designed to simulate extreme loading conditions that can occur in the field. Therefore, this experimental setup simulates a single wheel load imparted onto a single crosstie.

These experiments were conducted to analyze and quantify the loading behavior at this interface by using a variety of load inputs while varying concrete crosstie fastening system components. The first series of experiments was performed to determine a relationship between the rail pad modulus and pressure distribution at the rail seat. The modulus of a rail pad is often considered to be a proxy for the stiffness of the pad. However, the modulus is a property of the material whereas stiffness is dependent on both the material properties and the boundary conditions of the component.

Another series of experiments was performed to compare two different elastic fastening system clip designs with respect to their ability to distribute pressure over the rail seat. For each series of experiments, various L/V force ratios were explored in an attempt to simulate a variety of rail vehicle and track interaction conditions that could occur at the wheel–rail interface. The overall objective of this experimentation was to determine a relationship between L/V force ratio and pressure distribution at the rail seat while varying different components of the fastening system. The effect of varying L/V force ratios is explained in the following sections, and the experimental protocol and results from the aforementioned experiments are presented.

Many variables can affect the L/V force ratio, including the track geometry (e.g., horizontal curvature), wheel–rail interface conditions and frictional properties, axle loads, railcar truck steering performance, and train speed (15). Researchers at UIUC suspect that a high concentration of field side loading could be seen on the high rail seat on a section of superelevated track with a train operating in an underbalanced condition and that, inversely, a field side concentration on the low rail seat would be expected for a train operating in an overbalanced condition.

Experimentation with Rail Pad Component

Concrete crosstie fastening systems typically include a single-layer or multilayer rail pad assembly (16). Part of this assembly includes a polymer rail pad, historically made of rubber or polyethylene, to attenuate the load and provide protection for the concrete rail seat (1). Given that concrete crosstie track is often more rigid than the traditional timber crosstie track, concrete crossties can impart

higher stresses onto the ballast. Ballast aggregates can then deteriorate to powdered material, which can foul the ballast layer and deteriorate support conditions (17). An important purpose of the rail pad as an individual component is to provide increased resiliency for the concrete crosstie system. The increased resiliency provides the advantages of dampening the loads experienced by the rolling stock and increasing passenger comfort (18). Rail pads are manufactured from a variety of materials and molded into different geometries. Their material properties and component geometries govern the modulus and stiffness values for a given design.

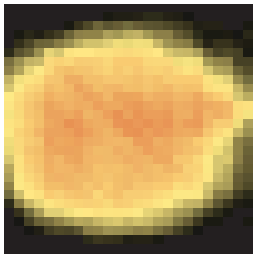
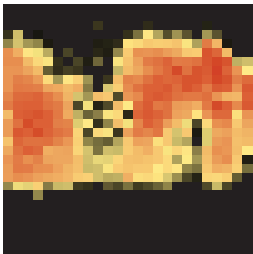
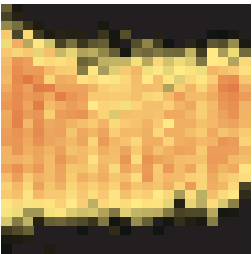
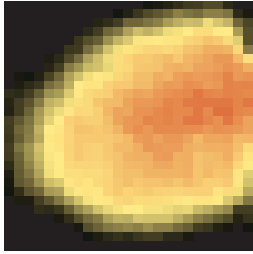
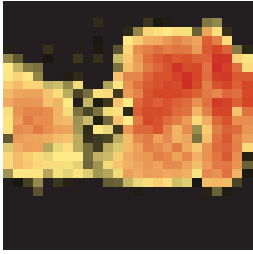
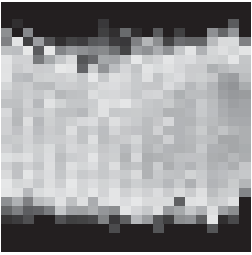
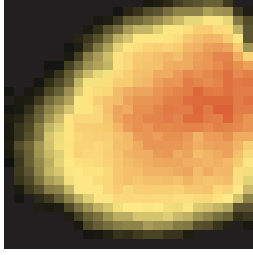
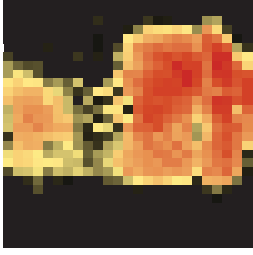
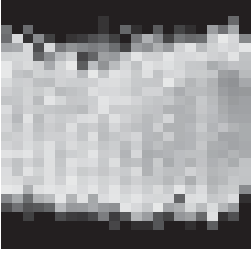
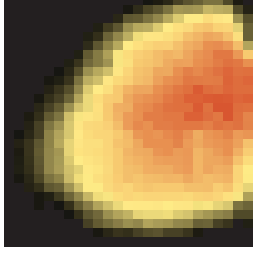
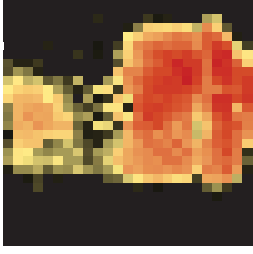
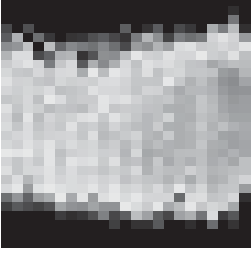
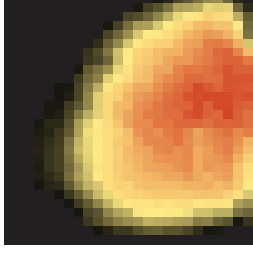
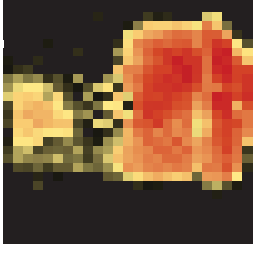
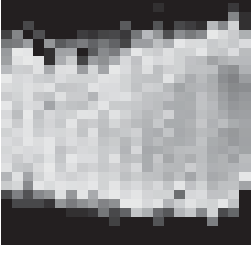
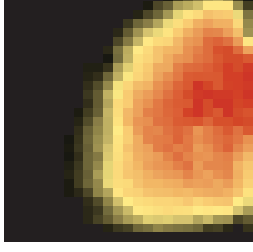
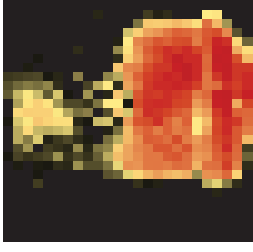
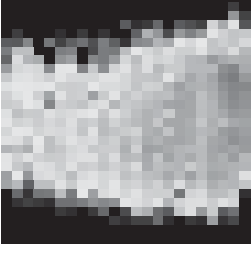
Part of the research being conducted at UIUC is investigating the effect of the rail pad's modulus on mitigating high loads imparted on the rail seat while continuing to protect the concrete rail seat. Researchers at UIUC are exploring the possibility that a rail pad of a lower modulus (i.e., softer) will distribute the applied load over a wider area of the concrete rail seat. Although a softer rail pad may better mitigate high-impact loads, its high resiliency allows for greater rail deflection, which can increase wear and fatigue of other components of the fastening system (1). The softer pad, in combination with the elastic clips commonly used in concrete crosstie fastening systems, can perform well in moderate traffic loading conditions (16). Under heavier loads, which are becoming increasingly common in North America, excessive lateral movement of the rail base and wear of the fastening system components can occur (16).

In performing AREMA Test 6 (Wear and Abrasion) with the PLTM, researchers at UIUC have seen this excessive lateral movement of the rail cause wear on the field side cast-in steel shoulder, which could potentially lead to gage widening. In both the 2008 and 2012 surveys of North American Class I railroads, shoulder and fastener wear or fatigue ranked second behind RSD as the most critical concrete tie problem (2, 3). Also, UIUC researchers are exploring the possibility that a rail pad with a higher modulus will help reduce the stress on the fastening system as a whole but will place a higher concentration of load on the concrete rail seat surface and in turn result in increased ballast pressures on the bottom of the crosstie (16).

An experiment was performed to compare the pressure distributions of a higher-modulus, medium-density polyethylene (MDPE) rail pad, a lower-modulus thermoplastic vulcanizate (TPV) rail pad, and a more commonly used two-part pad assembly made up of a nylon 6-6 abrasion plate and a 95 Shore A thermoplastic polyurethane pad. The MDPE and TPV rail pads used were cast with a flat surface specifically for this experiment to remove variation in pad geometry. The MDPE pad had a Shore hardness of 60 on the D scale, with a flexural modulus of 120,000 psi (827.4 N/mm²). The TPV pad had a Shore hardness of 86 on the A scale, with an approximate flexural modulus of 15,000 psi (103.4 N/mm²; this value is based on a TPV with a similar Shore hardness of 87A). Although the numerical value for the TPV rail pad Shore hardness is higher than that of the MDPE, the Type A scale is used for softer plastic materials, whereas the Type D is used for harder plastic materials. In this instance, the value of 60 for the Type D scale indicates a harder material than the values of 86 and 95 for the Type A scale.

Loading conditions were consistent for the three series of experiments: a constant vertical load of 32,500 lb (144.6 kN) and corresponding lateral loads based on the L/V force ratios being simulated. This magnitude of vertical load was chosen because it is the same value as that specified for the AREMA Test 6 (Wear and Abrasion), which is designed to simulate a heavy-axle freight car negotiating a sharp curve (6). For comparison of the relative performance of the three rail pad components, the maximum loaded frame per L/V force ratio was identified and obtained for each pad (Table 1).

TABLE 1 Rail Seat Pressure Distributions for Rail Pad Assemblies Under Varying L/V Force Ratios

L/V Force Ratio	TPV		MDPE		Two-Part Assembly	
	Gage	Field	Gage	Field	Gage	Field
0.25						
0.44						
0.48						
0.52						
0.56						
0.60						

NOTE: Pressure [psi (kPa)]:

0	500 (3,447)	1,000 (6,895)	1,500 (10,342)	2,000 (13,790)	2,500 (17,237)	3,000 (20,684)	3,500 (24,132)	4,000 (27,579)
---	----------------	------------------	-------------------	-------------------	-------------------	-------------------	-------------------	-------------------

TABLE 2 Results of Rail Pad Assembly Experiment

Parameter	L/V Force Ratio 0.25 by Pad Assembly			L/V Force Ratio 0.44 by Pad Assembly			L/V Force Ratio 0.48 by Pad Assembly		
	MDPE	TPV	Two-Part Pad	MDPE	TPV	Two-Part Pad	MDPE	TPV	Two-Part Pad
Vertical (kips)	32.50	32.50	32.50	32.50	32.50	32.50	32.50	32.50	32.50
Lateral (kips)	8.13	8.13	8.13	14.30	14.30	14.30	15.60	15.60	15.60
Contact area (in. ²)	20.09	28.75	24.73	19.31	27.93	23.96	19.12	27.25	23.91
Peak pressure (psi)	3,213	2,139	2,460	3,469	2,573	2,821	3,546	2,800	2,877
Contact area over 3,000 psi (in. ²)	0.34	0	0	1.55	0	0	2.32	0	0

NOTE: 1 kip = 4.45 kN; 1 in.² = 6.45 cm²; 1 psi = 6.89 kPa.

Table 2 is a compilation of the results from this series of experiments. The data collected for each rail pad component are presented side by side according to the *L/V* force ratio to show the difference in pressure distribution for the various materials under identical loading conditions. Figure 2, *a*, *b*, and *c*, shows plots of the average pressure per column of data from the MBTSS along the width of the sensor on the rail seat for the TPV, MDPE, and two-part pad assemblies, according to the *L/V* force ratio.

This experiment shows that the MDPE rail pad distributed the same applied load over a noticeably smaller area of the rail seat than the low-modulus TPV rail pad or two-part pad assembly. For an *L/V* force ratio of 0.25, the contact area of the load for the high-modulus MDPE rail pad was 20.09 in.² (129.61 cm²), only 70% of the amount of 28.75 in.² (185.48 cm²) of contact area recorded for the low-modulus TPV rail pad under the same load and only 81% of

the amount of 24.73 in.² (159.55 cm²) of the contact area for the two-part pad assembly. Peak pressures for each of the three pad assemblies occurred during the *L/V* force ratio of 0.60, since the same vertical load was being applied to smaller contact areas. Of the three pad assemblies used in the experimentation, the highest peak pressure recorded was for the MDPE rail pad, with a value of 4,096 psi (28,240 kPa). This value is approximately 20% higher than the peak pressure of 3,400 psi (23,440 kPa) recorded for the TPV rail pad and 23% higher than the 3,325 psi (22,930 kPa) recorded for the two-part pad assembly. The MDPE pad distributed this same load over 11% less of the rail seat surface than did the TPV rail pad and 17% less than did the two-part pad assembly; this distribution difference resulted in the higher peak pressures. Furthermore, although the MDPE rail pad had a smaller total contact area, it had a larger amount of area loaded at higher pressures than did the two other pad

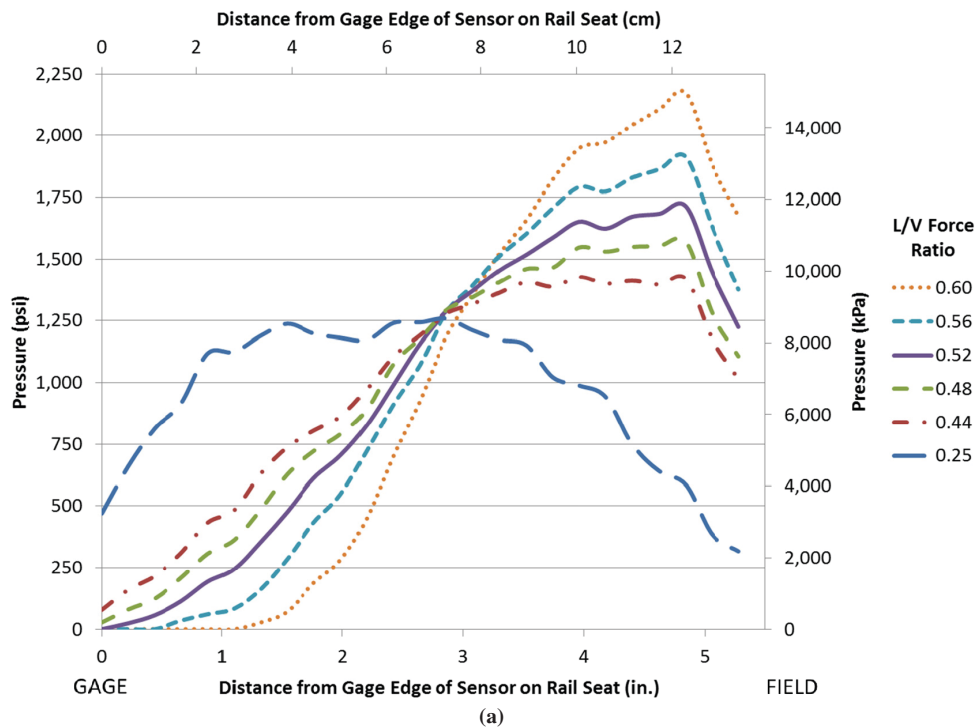


FIGURE 2 Average pressure distributions for (a) TPV rail pad. (continued)

L/V Force Ratio 0.52 by Pad Assembly			L/V Force Ratio 0.56 by Pad Assembly			L/V Force Ratio 0.60 by Pad Assembly		
MDPE	TPV	Two-Part Pad	MDPE	TPV	Two-Part Pad	MDPE	TPV	Two-Part Pad
32.50	32.50	32.50	32.50	32.50	32.50	32.50	32.50	32.50
16.90	16.90	16.90	18.20	18.20	18.20	19.50	19.50	19.50
19.02	25.75	23.86	18.63	23.96	23.38	17.76	21.30	23.38
3,721	2,925	2,990	3,838	3,162	3,201	4,096	3,400	3,325
2.86	0	0	3.44	0.53	0.10	4.11	1.74	0.29

components used, as is evident in the rows showing contact area over 3,000 psi (20,680 kPa) (Table 2).

In Figure 2, *a*, *b*, and *c*, the increase of loading into the field side of the rail seat as the *L/V* force ratio increases can be seen for all three rail pad assemblies. In Figure 2*c*, a wider range of more uniformly incremented *L/V* force ratios is presented to better show the transfer of the pressure distributed toward the field side of the rail seat. In all three instances, the decrease of pressure in the area immediately adjacent to the field side shoulder is likely due to the gap beneath the insulator post beyond the width of the base of the rail. The shape of the curves for each experiment could be due to variable material geometry or properties, which can in turn govern the rail base rotation, of each rail pad material under increasing *L/V* force ratios.

Additional experimental replicates are needed to gain further insight on the shape of the curve on an average rail seat. The curves

for the TPV pad are similar to the theoretical triangular distribution pattern noted in previous research on concrete cross-tie rail seat stress (4). This finding could be due to the fact that the lower modulus of the TPV pad allows the base of the rail to rotate more under increased lateral loads. The higher-modulus MDPE pad, however, would allow less rotation of the rail base; this condition resulted in the distributions shown in Figure 2*b*. The possibility that a rail pad component with a lower modulus could allow greater rotation of the base of the rail is supported by the fact that the largest decrease in contact area under increasing *L/V* force ratio occurred for the TPV rail pad. A decrease of approximately 26% of contact area occurred between the *L/V* force ratios of 0.25 and 0.60 for the TPV rail pad as compared with 12% and 5% for the MDPE pad and two-part assembly, respectively.

The behavior of the commonly used two-part pad assembly can be seen as a hybrid of the higher-modulus MDPE pad and the

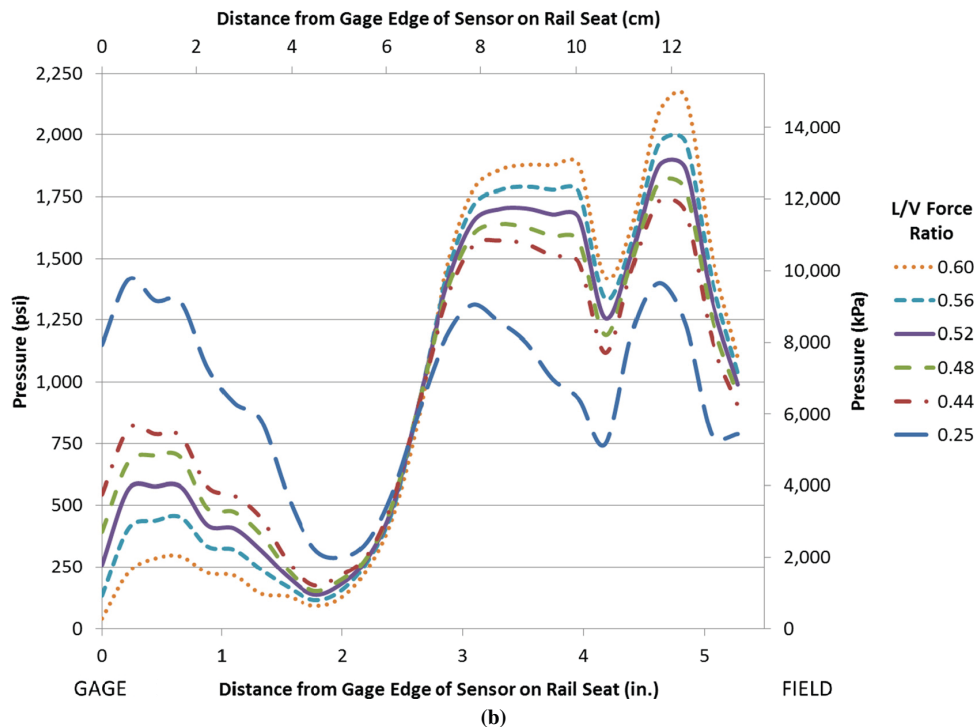


FIGURE 2 (continued) Average pressure distributions for (b) MDPE rail pad. (continued on next page)

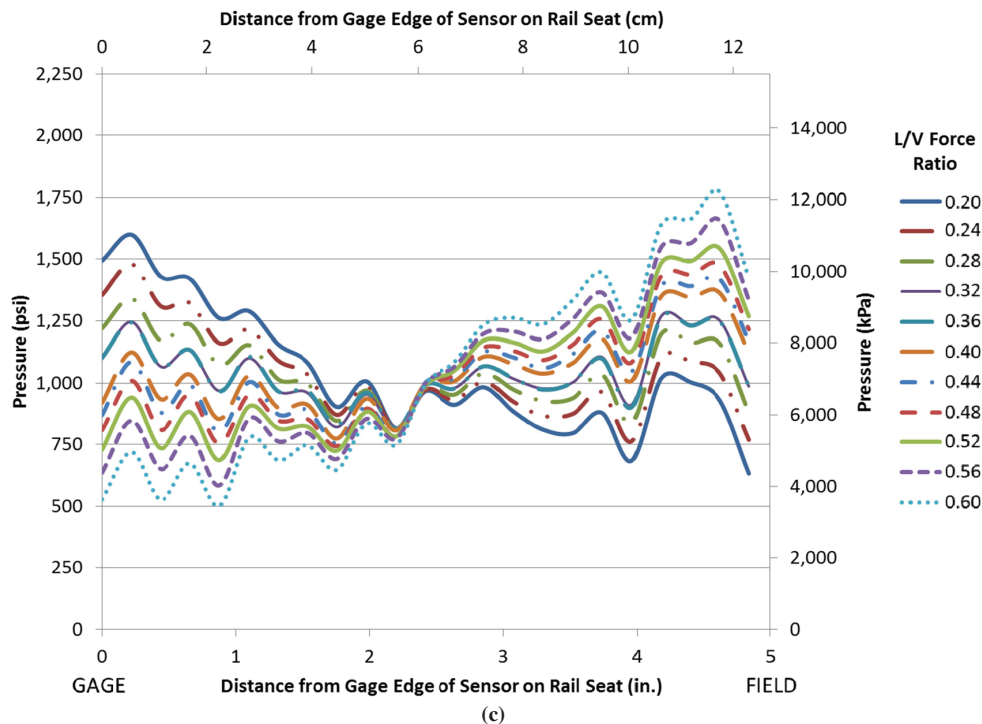


FIGURE 2 (continued) Average pressure distributions for (c) two-part pad assembly.

lower-modulus TPV pad. The peak pressure values were on average closer to those of the TPV pad, while the least change in contact area under increasing L/V force ratio of the three pad components used in the experimentation was found. However, the ability of the two-part pad assembly to resist rotation of the rail base more closely mirrored that of the MDPE pad; the decrease in contact area under increasing L/V force ratios was more similar between these two components than to the TPV rail pad. This similarity can also be seen in Figure 2, where under an L/V force ratio of 0.60, both the MDPE and two-part pad assemblies retained contact on the gage side of the rail seat, whereas this area under the TPV rail pad became unloaded.

For this experiment, and the following clip component experiment, data were not collected in the area immediately adjacent to the gage side of the rail seat. Figure 2, *a*, *b*, and *c*, shows that the width of the sensor on the x -axis is less than the actual full width of the rail seat used for experimentation. This finding is due to the need to protect the MBTSS by allowing the conductive leads extending from the pressure-sensitive area of the sensor to lie flat on the rail seat rather than bending that area over the base of the rail. Bending of the sensor around the base of the rail was found to cause damage to the sensor in earlier experimentation. Sacrificing data on the gage side was accepted by the researchers at UIUC, since the pressures near the field side were the primary target of this investigation.

From this experiment, it can be seen that a direct relationship exists between a high rail pad modulus and concentrated loading of the rail seat. Furthermore, a highly concentrated loading of the rail seat could lead to crushing of the concrete surface, although the peak pressure values recorded in this laboratory experimentation did not approach the AREMA-recommended minimum 28-day-design compressive strength of concrete used for concrete ties of 7,000 psi (48,260 kPa) (6). It is also possible that highly concentrated loads

could be seen in the field because although the maximum vertical load explored in this laboratory experimentation was only 32.5 kips (144.56 kN), wheel impact load detector sites in revenue service can record loads of greater than 100 kips (444.82 kN) (19). It is likely that a load of this magnitude would produce pressures on the rail seat in excess of 7,000 psi (48,260 kPa).

Another parameter that could affect the rail pad's ability to evenly distribute pressure is dynamic load attenuation. Under repeated loading cycles, such as those imparted by unit coal trains, the inability of the pad to fully recover elastically between axles could lead to changes in the distribution of pressure on concrete rail seats. Investigation into repeated loadings of rail pads could also lead to discussion of the effect of wear life of this component on rail seat pressure distribution.

Experimentation with Fastening Clip

Fastening systems for concrete crossties serve the primary purposes of providing vertical, lateral, and longitudinal restraint of the rail and providing load attenuation. A variety of clip designs and rail pad materials result in concrete crosstie and elastic fastening systems with unique stiffness characteristics, which result in a variety of specialized performance capabilities (16). An experiment was performed to investigate pressure distribution on the rail seat while varying the clip component of a concrete crosstie fastening system. Two common North American fastening system clip designs were used for this experiment; they will be referred to as Clip A and Clip B (Figure 3). The design clamping force for Clip A was 4,750 lb (21.1 kN), with a spring rate of 8,223 lb/in. (14.4 kN/cm). The design clamping force for Clip B was 5,500 lb (24.5 kN), with a spring rate of 6,286 lb/in. (11.0 kN/cm). The spring rate values

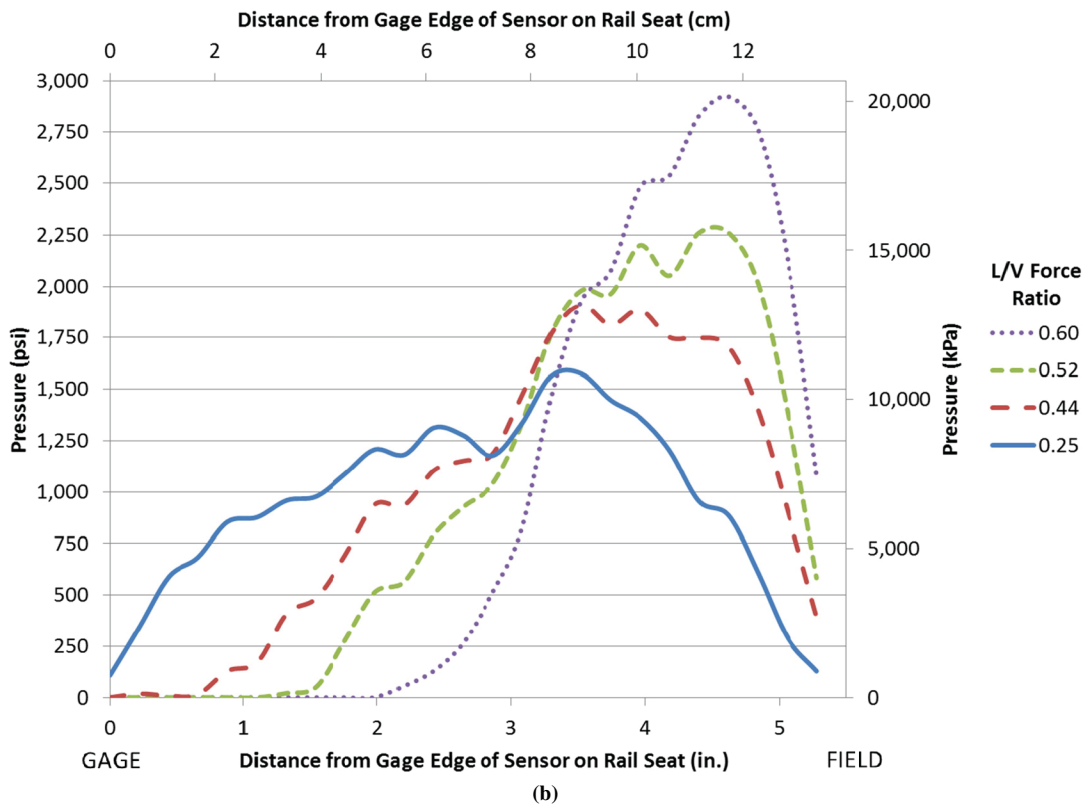
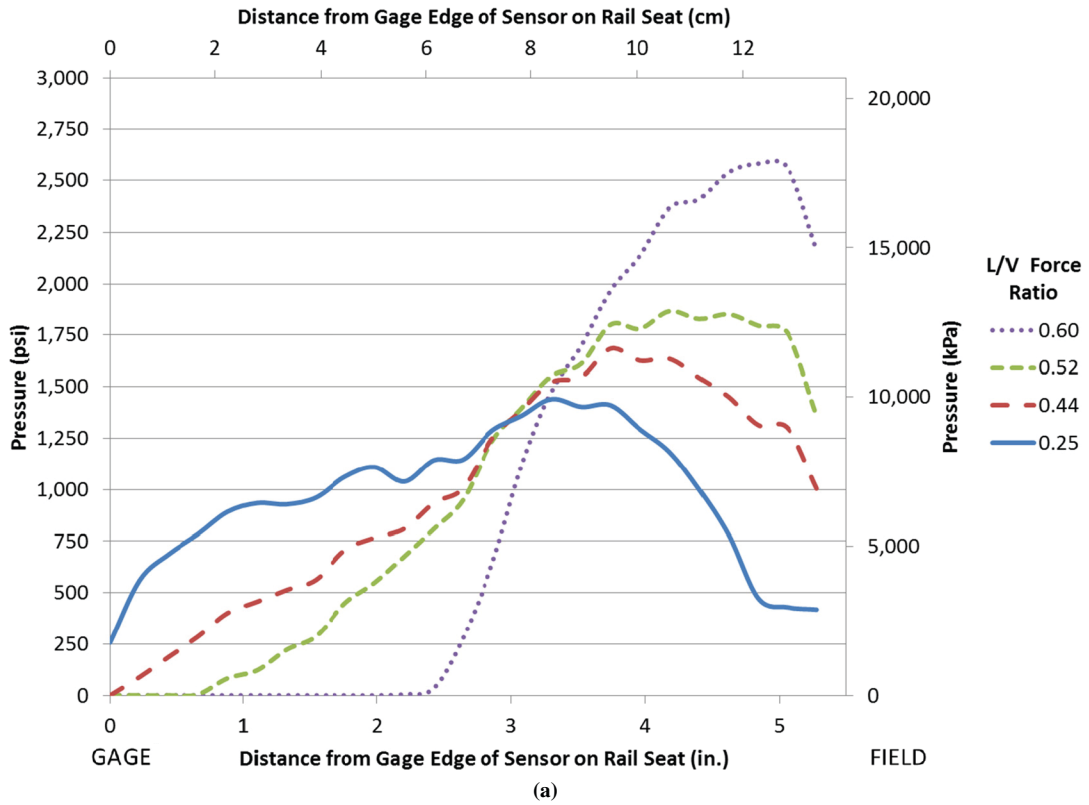


FIGURE 3 Average pressure distributions for (a) Clip A and (b) Clip B.

were determined from the manufacturer's design clamping force at a given deflection.

The same two-part rail pad assembly was used for each clip to hold that variable constant. A different concrete crosstie was used for each respective clip experiment, because the cast-in steel shoulder design for each fastening system was different. This feature could result in variability in pressure distributions due to minor differences in the concrete rail seat profile; however, these differences should not be significant.

Loading conditions were consistent for this experiment: a constant vertical load of 32,500 lb (144.6 kN) and corresponding lateral loads based on the L/V force ratios simulated. Four L/V force ratios were used for this experiment, ranging from 0.25 to 0.60. For the comparison of the relative performance of the two clip designs, the maximum loaded frame per L/V force ratio was obtained for each clip (Table 3). Table 4 is a summary of results from these maximum loaded frames. Figure 3a is a plot of the average pressure per column of data from the MBTSS along the width of the sensor on the rail seat for Clip A according to the L/V force ratio. Figure 3b is the same plot of data collected during the experiment for Clip B.

Results from this experiment show a lower magnitude of variability between these two fastening system components than results from earlier experimentation with different rail pad moduli. The general trend was that Clip A distributed the pressure over a slightly larger area, thus producing lower peak pressure values. The greatest difference in contact area between the two clips was 2.61 in.² (16.84 cm²), at an L/V force ratio of 0.52. At the most extreme L/V force ratio of the experiment, the difference in peak pressures was only 274 psi (1,890 kPa); the value for Clip B was 7.2% higher than that of Clip A.

A notable difference between the results from the two clips is the shape of the pressure distributions. It appears that the geometry of each clip affects where load is concentrated on the rail seat, but no replicates with additional crossties or fastening systems have been conducted. In all of the pressure distribution frames for Clip B, a central area of concentrated pressure is noted, and the design of this clip is such that there is one point of contact between the clip and the insulator resting on the rail base, as can be seen in Table 3. For Clip A distributions, the peak pressures appear to be concentrated over a wider area of the rail seat and not on a single area like Clip B. This finding appears logical, since the design of Clip A has two points of contact between the clip and insulator, as can be seen in Table 3. This concept is also supported by the fact that the Clip B experiments showed that higher peak pressures were imparted into the rail seat, whereas Clip B had smaller contact areas than Clip A for all but the L/V force ratio of 0.60. Whether these same pressure distributions are seen in the field is not yet known; researchers at UIUC intend to investigate this aspect through future field experimentation.

CONCLUSIONS AND FUTURE WORK

The following conclusions can be drawn from the analysis of data collected in these preliminary experiments with MBTSS:

- Lower-modulus rail pads distribute rail seat loads over a larger contact area and reduce peak pressure values and mitigate highly concentrated loads at this interface.
- Higher-modulus rail pads distribute rail seat loads in more highly concentrated areas; this distribution possibly leads to localized crushing of the concrete surface under extreme loading events.

- A more commonly used two-part pad assembly composed of both higher- and lower-modulus materials can provide the benefits of reducing peak pressure values and maintaining a more constant contact area under increasing L/V force ratios and reducing rail base rotation.

- A lower L/V force ratio of the resultant wheel load distributes the pressure over a larger contact area.
- A higher L/V force ratio of the resultant wheel load causes a concentration of pressure on the field side of the rail seat; the result is higher peak pressures.
- The design of the clip component of the fastening system affects the shape of the pressure distribution on the rail seat.
- No large differences in the values for peak pressure or contact area were seen between the two clip designs used in this experimentation.

Given the projected increase in the use of concrete crossties in the North American railroad industry, research will continue at UIUC to develop a comprehensive laboratory and field instrumentation plan to better understand interactions at this interface. The experiments described here were theoretical in nature; the loading conditions were chosen by researchers on the basis of expert opinion and working knowledge of rail seat loads.

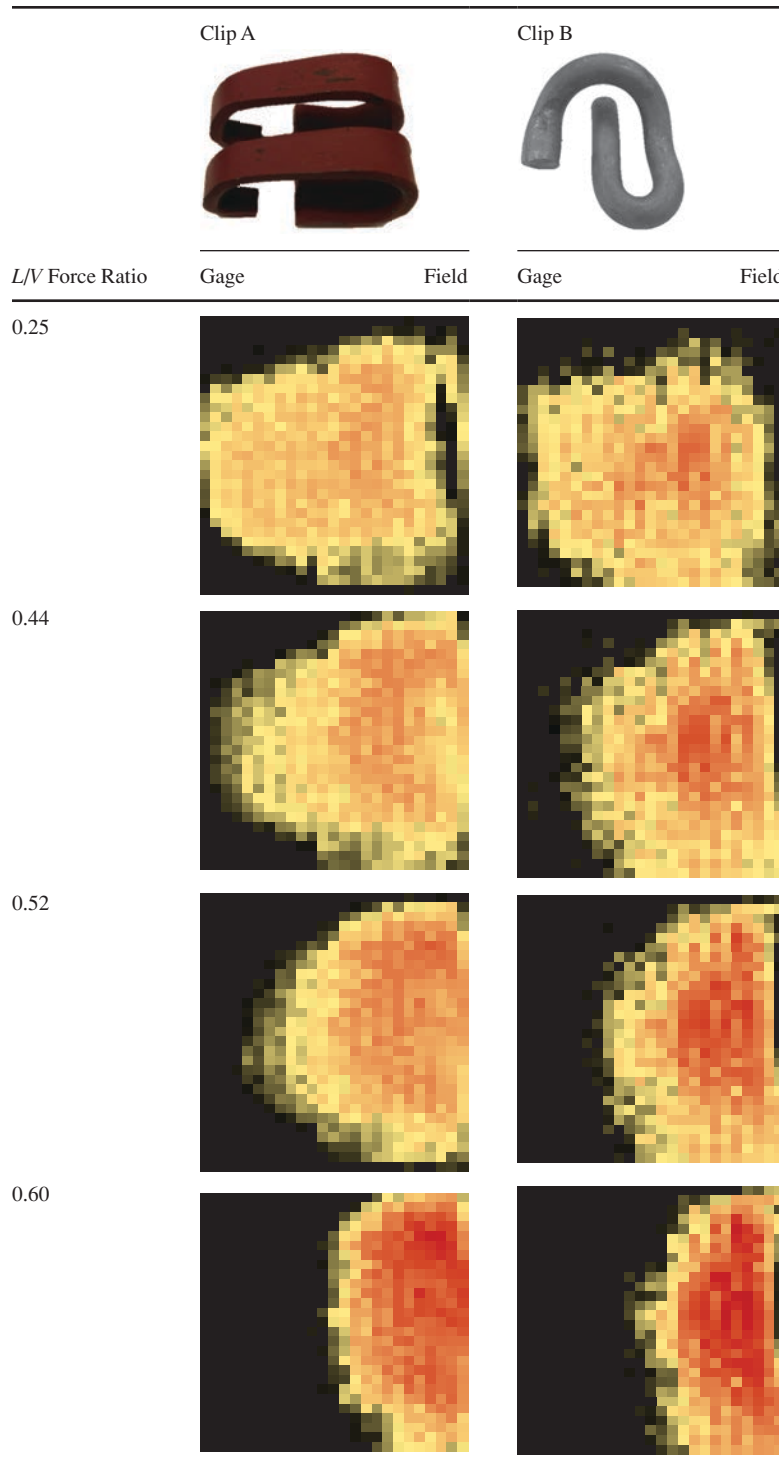
Future laboratory experimentation planned by researchers at UIUC includes installing MBTSS on rail seats of concrete crossties with various models of fastening systems to further view the effect that variations in clip design have on rail seat pressure distribution. Additional rail pad component experimentation will take place to better understand the material properties of this component and the effect it has on mitigating rail seat pressures. Experiments with rail pads of varying thicknesses will also be performed to better understand their effect on rail seat pressure distribution, since rail pad thickness was not a variable in the initial pad component experimentation. Since a load applied to a larger contact area appears to result in lower peak pressure values, experiments will also be conducted on crossties with various rail seat dimensions and degrees of deterioration or repair by using epoxy or other materials. Future experimentation with more intermediate values of the L/V force ratio, such as those seen in Figure 2c, will aid the understanding of the transition of pressure from the gage to field side under an increasing lateral component of the resultant wheel load.

Having run several preliminary experiments in the laboratory, as well as having developing a means to modify and protect the sensor for more accurate data collection, researchers at UIUC plan to instrument MBTSS on concrete crossties in the field. Field experimentation will allow analysis of actual loading conditions on the concrete rail seat surface with varying configurations of train loads, speeds, and track geometry. Another variable that it is proposed to investigate in field testing is the effect of top-of-rail friction modification on the distribution of loads onto the rail seats of concrete crossties.

Field experimentation will also play a crucial role in guiding the future of laboratory experimentation. A good working relationship between field data and experimental data is expected as the pressure distribution data collection process is refined and field conditions are better simulated in the laboratory.

In summary, the use of MBTSS is a feasible means to instrument concrete crossties to measure rail seat pressure distributions. Furthermore, results from this work will be leveraged, since the data collected from MBTSS in the laboratory and field will be used as an input for rail seat loads into finite element model analysis of the concrete crosstie and fastening system currently being performed at UIUC.

TABLE 3 Rail Seat Pressure Distributions for Fastening Clips Under Varying L/V Force Ratios



NOTE: Pressure [psi (kPa)]:

0	500 (3,447)	1,000 (6,895)	1,500 (10,342)	2,000 (13,790)	2,500 (17,237)	3,000 (20,864)	3,500 (24,132)	4,000 (27,579)
---	----------------	------------------	-------------------	-------------------	-------------------	-------------------	-------------------	-------------------

TABLE 4 Results of Fastening Clip Experiment

Parameter	L/V Force Ratio by Clip Design							
	0.25		0.44		0.52		0.60	
	A	B	A	B	A	B	A	B
Vertical (kips)	32.50	32.50	32.50	32.50	32.50	32.50	32.50	32.50
Lateral (kips)	8.13	8.13	14.30	14.30	16.90	16.90	19.50	19.50
Contact area (in. ²)	28.36	27.59	26.57	24.54	23.62	21.01	16.55	17.18
Peak pressure (psi)	2,188	2,744	2,327	3,067	2,872	3,385	3,809	4,083
Contact area over 3,000 psi (in. ²)	0	0	0	0.24	0	0.92	2.13	3.53

ACKNOWLEDGMENTS

This research was funded by Amsted RPS–Amsted Rail, Inc., and FRA, U.S. Department of Transportation. J. Riley Edwards was supported in part by grants to the UIUC Rail Transportation and Engineering Center from Canadian National Railway, CSX Corporation, Hanson Professional Services, Norfolk Southern, and the George Krambles Transportation Scholarship Fund. For direction, advice, and resources the authors thank Jose Mediavilla of Amsted RPS; Brent Wilson of Amsted Rail; Mauricio Gutierrez of GIC Ingeniería y Construcción, Mexico; Jerry Rose and Jason Stith of the University of Kentucky; and Vince Carrara of Tekscan, Inc. The authors also thank Marc Killian, Tim Prunkard, and Don Marrow of the University of Illinois at Urbana–Champaign for their assistance in laboratory experimentation and graduate students Ryan Kernes, Brandon Van Dyk, Brennan Caughron, Sam Sogin, and Amogh Shurpali for their peer review, editing, and valuable input.

REFERENCES

- International Heavy Haul Association. *Guidelines to Best Practices for Heavy Haul Railway Operations, Infrastructure Construction, and Maintenance Issues*. D. & F. Scott Publishing, Inc. North Richland Hills, Tex., 2009, Chaps. 1, 3, and 5, pp. 1-59, 3-67, 3-72, 5-2, and 5-6.
- Zeman, J. C. *Hydraulic Mechanisms of Concrete-Tie Rail Seat Deterioration*. MS thesis. University of Illinois at Urbana–Champaign, Urbana, 2010, Chaps. 1, 2, and 3.
- Van Dyk, B. J., M. S. Dersch, and J. R. Edwards. *International Concrete Crosstie and Fastening System Survey—Final Results*. University of Illinois at Urbana–Champaign, Urbana, 2012.
- Marquis, B. P., M. Muhlanger, and D. Y. Jeong. Effect of Wheel/Rail Loads on Concrete Tie Stresses and Rail Rollover. *Proc., ASME 2011 Rail Transportation Division Fall Technical Conference*, Minneapolis, Minn., American Society of Mechanical Engineers, New York, 2011, pp. 1–3.
- Rhodes, D. How Resilient Pads Protect Concrete Sleepers. *Railway Gazette International*, Feb. 1988, p. 85.
- AREMA Manual for Railway Engineering*. American Railway Engineering and Maintenance-of-Way Association, Lanham, Md., 2009, Vol. 1, Chap. 30.
- Wnek, M. A., E. Tutumluer, M. Moaveni, and E. Gehringer. Investigation of Aggregate Properties Influencing Railroad Ballast Performance. In *Transportation Research Record: Journal of the Transportation Research Board*, No. 2374, Transportation Research Board of the National Academies, Washington, D.C., 2013, 180–189.
- Lake, M., L. Ferreira, and M. Murray. Using Simulation to Evaluate Rail Sleeper Replacement Alternatives. In *Transportation Research Record: Journal of the Transportation Research Board*, No. 1785, Transportation Research Board of the National Academies, Washington, D.C., 2002, pp. 58–63.
- Giannakos, K. Comparison of Magnitude of Actions on Track in High-Speed and Heavy-Haul Railroads: Influence of Resilient Fastenings. In *Transportation Research Record: Journal of the Transportation Research Board*, No. 2289, Transportation Research Board of the National Academies, Washington, D.C., 2012, pp. 70–77.
- Rose, J. G., and J. C. Stith. *Pressure Measurements in Railroad Trackbeds at the Rail/Tie Interface Using Tekscan Sensors*. University of Kentucky, Lexington, 2004, pp. 1–20.
- Kerchof, B., and H. Wu. Causes of Rail Cant and Controlling Cant Through Wheel/Rail Interface Management. *Proc., Annual Conference of the American Railway Engineering and Maintenance-of-Way Association*, Chicago, Ill., American Railway Engineering and Maintenance-of-Way Association, Lanham, Md., 2012.
- Costello, S. B., A. S. Premathilaka, and R. C. M. Dunn. Stochastic Rail Wear Model for Railroad Tracks. In *Transportation Research Record: Journal of the Transportation Research Board*, No. 2289, Transportation Research Board of the National Academies, Washington, D.C., 2012, pp. 103–110.
- Andersson, E., N. G. Nilstam, and L. Ohlsson. Lateral Track Forces at High Speed: Curving Comparisons of Practical and Theoretical Results of Swedish High Speed Train X2000. *Vehicle System Dynamics: International Journal of Vehicle Mechanics and Mobility*, Vol. 25, Suppl. 1, 2007, pp. 37–52.
- Gutierrez, M. J., J. R. Edwards, C. P. L. Barkan, B. Wilson, and J. Mediavilla. Advancements in Fastening System Design for North American Concrete Crossties in Heavy Haul Service. *Proc., Annual Conference of the American Railway Engineering and Maintenance-of-Way Association*, Orlando, Fla., American Railway Engineering and Maintenance-of-Way Association, Lanham, Md., 2010, p. 5.
- Iwnicki, S. (ed.). *Handbook of Railway Vehicle Dynamics*. CRC Press, Boca Raton, Fla., 2006.
- Hay, W. W. *Railroad Engineering*, 2nd ed. John Wiley & Sons, Inc., New York, 1982, Chap. 23, pp. 471–473.
- Moaveni, M., S. Wang, J. M. Hart, E. Tutumluer, and N. Ahuja. Evaluation of Aggregate Size and Shape by Means of Segmentation Techniques and Aggregate Image Processing Algorithms. In *Transportation Research Record: Journal of the Transportation Research Board*, No. 2335, Transportation Research Board of the National Academies, Washington, D.C., 2013, pp. 50–59.
- Giannakos, K., and A. Loizos. Evaluation of Actions on Concrete Sleepers as Design Loads: Influence of Fastenings. *International Journal of Pavement Engineering*, Vol. 11, No. 3, 2010, p. 197–213.
- Trosino, M. J. Load Spectra for High-Speed Rail in Mixed Service. Presented at 90th Annual Meeting of the Transportation Research Board, Washington, D.C., 2011.

The published material in this paper represents the position of the authors and not necessarily that of the U.S. Department of Transportation.

The Railway Maintenance Committee peer-reviewed this paper.